Record High Magnetic Anisotropy in Three Coordinate Mn^{III} and Cr^{II} Complexes: A Theoretical Perspective

*Arup Sarkar, Reshma Jose, Harshit Ghosh and Gopalan Rajaraman**

Department of Chemistry, Indian Institute of Technology Bombay, Mumbai- 400076, Maharashtra, India

Keywords: Low-coordinate, *Ab initio*, NEVPT2, Zero-field Splitting, Spin-vibronic coupling

ABSTRACT: *Ab initio* calculations performed in two three-coordinate complexes $[Mn\{N(SiMe_3)_2\}_3]$ (1) and $[K(18\text{-crown-}6)(Et_2O)_2][Cr\{N(SiMe_3)_2\}_3]$ (2) reveal record-high magnetic anisotropy with the *D* values -64 cm^{-1} and -15 cm^{-1} respectively, enlisting d^4 ion back in the race for single-ion magnets. For the first time, a detailed spin-vibrational analysis was performed in **1** and **2** that suggests a dominant under barrier relaxation due to flexible coordination sphere around the metal ion offering design clues for low coordinate transition metal SIMs.

Introduction

Single-Molecule Magnets (SMMs) have become a fascinating research area as this class of molecules exhibit magnetization just like permanent magnets below a critical temperature defined as blocking temperature T_B.[1] An important parameter associated with the blocking temperature is the barrier height for magnetization reversal (U_{eff}) which is correlated to the magnetic moment of different microstate and the nature of anisotropy. While in lanthanide complexes, the first-order spin-orbit coupling (SOC) is strong enough to produce large barrier heights,[2] in transition metal (TM) systems spin-orbit coupling is generally weak, leading to relatively smaller anisotropy which is reflected in the axial zero-field splitting parameter (*D*) which can be tuned at will using ligand field.[3]

There are several challenges in enhancing the blocking temperature T_B in SMMs as several relaxation mechanisms other than the Orbach process spoil the direct correlation of T_B to U_{eff} values. Among others, quantum tunneling of magnetization (QTM) and spin-phonon/vibrational-mode relaxation mechanisms are a prominent source of relaxation, as shown in recent years by various groups.[4] Earlier research in the SMM area was focused on increasing the total spin (*S*) of the complexes by increasing the number of metal centers. After the discovery of a very small U_{eff} barrier in $\{Mn_{19}\}$ cluster possessing record high ground state *S* value, it becomes clear that increasing the number of metal centers or *S* value diminishes the axial anisotropy (*D* term) as evident from the equation proposed originally by Abragam and Bleaney[5] and adapted in *ab initio* calculations later on. For this reason, mononuclear TM complexes gained significant attention leading to the birth of several single-ion magnets (SIMs) based on the low coordination number such as Fe(II/I), Ni(II), and Co(II), exhibiting very large U_{eff} values.[6]

In the early years of SMMs, the focus has been on transition metal cluster particularly that of Mn(III) ions, as this offer an easy source of negative *D* parameter for the chemists and unearthed numerous SMMs albeit with smaller U_{eff}/T_B values. [1a, 7] The Mn(III) ions are very robust and can be easily incorporated in cluster aggregation, and are relatively redox stable[6a] but exhibit only small *D* values of the order of ~|5| cm^{-1}. [8] While several low-coordinate transition metal ions were pursued recently for potential SMMs, Mn(III) has not been studied in detail, perhaps due to the perception that the expected *D* values are rather small.[8] Apart from U_{eff} values, the blocking temperature is an important criterion which is often very small. This suggests that apart from the QTM effect, spin-vibrational relaxations are at play in such systems.[4] How these effects manifest in these complexes are not fully understood.

To ascertain complexes that exhibit large negative *D* values and also to correlate the relaxation mechanism to spin-vibrational coupling, we undertake theoretical studies based on multi-configurational *ab initio* calculations SA-CASSCF/NEVPT2 using the ORCA suite.[9] Here, we have studied in detail two three-coordinate d^4 systems Mn(III) and Cr(II): $[Mn\{N(SiMe_3)_2\}_3]$[10] (**1**) and $[K(18\text{-crown-}6)(Et_2O)_2]$ $[Cr\{N(SiMe_3)_2\}_3]$[11] (**2**) using their reported X-ray structure. Our NEVPT2 calculations yield a record axial *D* value of -64 cm^{-1} and -15 cm^{-1} for **1** and **2**, respectively, with a negligible *E*/*D* value. The *D* value computed for both complexes is larger than any examples reported to-date and suggests a potential SMMs characteristic for these robust building block metal ions.

Computational Details

All the *ab initio* single point calculations have been performed using ORCA 4.0.0 program.[9] DKH (Douglas-Kroll-Hess) Hamiltonian was used to account for the scalar relativistic effect. DKH

contracted versions of the basis sets were used during the calculations- DKH-def2-TZVP for Mn, Cr, Si; DKH-def2-TZVP(-f) for N and DKH-def2-SVP for the rest of the atoms. During the orbital optimization step in SA-CASSCF (state-averaged complete active space self-consistent field) method, 4 metal electrons in 5 metal d-orbitals were taken into consideration and optimized with 5 quintet and 35 triplet roots for Mn(III) and Cr(II) metal centers. Additional calculations have also been carried out with 5 quintets, 45 triplet roots, and 5 quintets, 35 triplet, and 22 singlet roots to check the effect of high-lying excited states on the Spin-Hamiltonian (SH) parameters. The addition of extra 10 triplet roots and 22 singlet roots marginally affect the SH parameters (see Table **S1** in ESI). NEVPT2 (N-electron valence perturbation theory second-order) calculation has also been performed on the top of converged SA-CASSCF wavefunction to include the dynamic electron correlation. Spin-orbit interaction was accounted with quasi-degenerate perturbation theory (QDPT) approach using SOMF (spin-orbit mean field) operator. Only spin-orbit contributions towards zero-field splitting were computed. Final Spin-Hamiltonian parameters were determined with effective Hamiltonian approach (EHA) formalism.[12] *Ab initio* ligand field theory (AILFT) calculations have also been performed to obtain the d-orbital energies.[13]

Geometry optimization and single point frequency calculations have been carried out in Gaussian 09 (Rev. D.01) program.[14] Hybrid unrestricted B3LYP-D2 functional was used for the DFT calculations along with Ahlrich's triple-ζ valence polarized (TZVP) basis set for Mn, Cr, Si, N and Ahlrich's spilt valence polarized (SVP) basis set for rest of the atoms.[15]

Result and Discussions

Complex **1** possesses a perfect D_{3h} symmetry as the three ∠N-Mn-N bond angles are 120.02°, 120.02° and 119.95° and the three Mn-N bond lengths are 1.89, 1889, and 1.89 (in Å unit). It was also noticed that the $\{MnN_3\}$ core was planar, and the bulky trimethylsilyl groups surrounded the central moiety stabilizes the low coordinate molecule from further coordination via steric arrangements (see Figure **1**). The NEVPT2-QDPT calculated major anisotropy axes, i.e., D_{zz} and g_{zz} axes, were found to be exactly perpendicular to the Mn-N_3 plane, i.e., exactly collinear with the C_3 axis, which describes the axial nature of anisotropy present in the molecule.

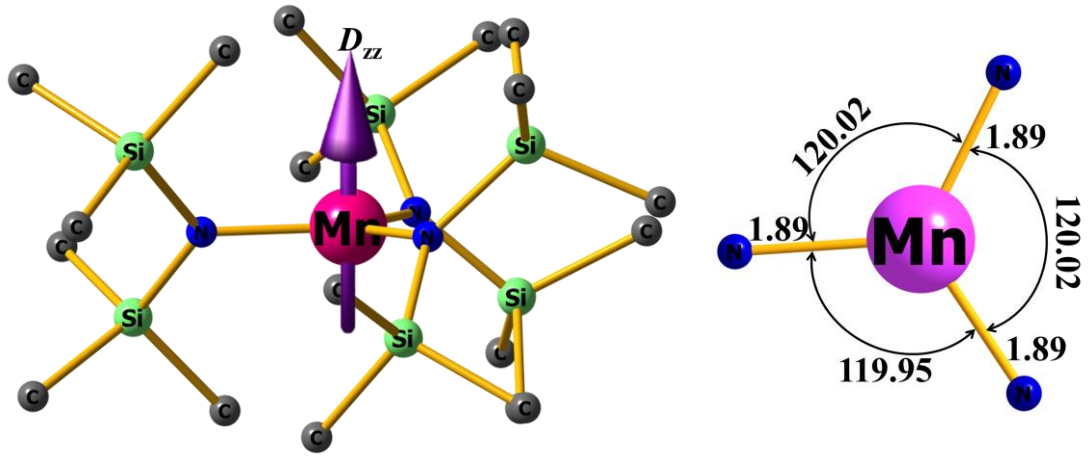

Figure 1: NEVPT2 computed D_{zz} axis of the molecule plotted on the X-Ray structure (left) and three Mn-N bond lengths (in Å) and ∠N-Mn-N angles (°) shown on the molecule (right). Colour code: Mn: pink, N: blue, Si: light green, C: dark grey. Hydrogens are omitted due to clarity.

A record axial zero-field splitting (ZFS) was found for this complex, showing a *D* value of -64 cm^{-1} with *E*/*D* estimated to be 0.0003, indicating strong easy-axis type anisotropy (see Table **1**) for complex **1**. A very similar geometry was observed in the Cr(II) analog, and the ∠N-Cr-N bond angles (123.9°, 115.81° and 120.29°) are not exactly similar and significantly deviated from D_{3h} symmetry. The *D* value for complex **2** is less than complex **1** due to these structural deviations and also smaller spin-orbit coupling constant (ζ) values of Cr(II) than Mn(III). For complex **2**, the *E*/*D* value is estimated to be 0.003, which is ten times larger than complex **1** (see Figure **S1** and Table **S1** in ESI).

The ground state electronic configuration of complex **1** is $d_z^{2\,1}d_{yz}^{1}d_{xz}^{1}d_{xy}^{1}d_{x^2-y^2}^{0}$, and this comprises 77% of the overall wavefunction. The major contribution (-62 cm^{-1}) towards the negative *D* value arises from the first excited state, which consists of $d_{xy} \rightarrow d_{x^2-y^2}$ (same M_L valued) electronic excitation and this excited state contribute ~97% of the overall *D* value (see Figure **2** and Table **S2** in ESI). Other electronic transitions were found to contribute negligibly to the overall *D* value. A very close analysis of the NEVPT2 states reveals that the first excited quintet state is only 19 cm^{-1} apart from the ground state and consequently results in a very strong second-order spin-orbit coupling. While the first excited state is the spin-allowed quintet, the second, third and fourth excited states arise from the spin-flipped triplet transitions. These three excited states consist of a mixture of $d_{xy} \rightarrow d_{xz}/d_{yz}$ and $d_{xy} \rightarrow d_{z^2}$ transitions (see Table **S2** in ESI). The computed g_x, g_y and g_z values are 1.67, 1.67 and 1.14 respectively for true spin S =2 and 0.00 0.00 and 5.14, respectively for pseudospin $\hat{S}$ =1/2 manifold. In the case of complex **2**, the first excited state contributes 96% (-14.4 cm^{-1}) towards the overall *D* value. Again, the *D* value is negative due to the coupling with the prominent first excited state involving the same M_L level $d_{xy} \rightarrow d_{x^2-y^2}$ electronic excitation (see Figure **S2** in ESI). Here one major difference of complex **2** from complex **1** is that due to

significant distortion from D_{3h} and lower ligand field of Cr(II), the first excited state is 756 cm^{-1} apart and the next three excited states are quintets (see Table **S3**). The computed g_x, g_y and g_z values are 1.97, 1.97, and 1.58 respectively for true spin S=2 and 0.00 0.00 and 6.351, respectively for pseudospin $\hat{S}$ =1/2 manifold.

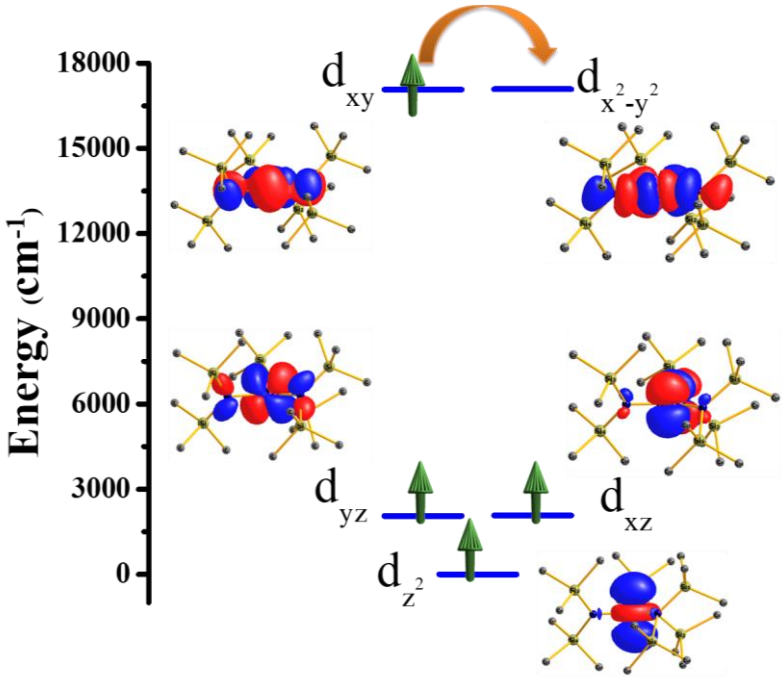

Figure 2: NEVPT2-LFT d-orbital diagram of complex **1**. The orange arrow indicates the first excited spin-allowed transition.

In the case of non-Kramers ions like in these two cases studied, the tunnel-splitting is generally larger, leading to faster relaxation via the QTM process. The tunnel-splitting strongly depends on the local symmetry and ligand field environment around the metal ion. The high symmetry present in complexes **1** and **2** leads to smaller tunnel splitting (see Figure **S3** and Table **S4** in ESI). The first excited pseudo-KDs is separated by 154 cm^{-1} in case of complex **1** and 45 cm^{-1} in case of

complex **2**. The multi-determinant nature of the ground state leads to mixing of the |+2⟩ and |-2⟩ states, and this is very prominent in complex **1** compared to **2** (see Table **S4**).

The static electronic picture is insufficient to describe the relaxation mechanism or the spin dynamics of the system. Recent reports of spin-vibronic coupling that describe the role of vibrational frequencies of a single molecule or of the surrounding lattice are very important to elucidate the dynamic scenario of SMMs.[4] In this regard, we have attempted to investigate the role of molecular vibrations occurring at low temperatures on the spin-orbit or *M*s levels in the two complexes. Therefore, we have performed frequency calculations (normal modes) on the X-ray structures of **1** and **2** using Density Functional Theory (DFT) methods (B3LYP-D2/TZVP, a similar vibrational pattern also found for the optimized geometries, see Table **S5** in ESI).

Here we have carefully analyzed five lower energy vibrational modes below 80 $cm^{-1,}$ and these are ν_1 45.1 (40.1), ν_2 45.8(46.2), ν_3 58.4(50.3), ν_4 70.3(58.8) and ν_5 72.9 (69.9) for complex **1** (**2**) (see Figure **S4** in ESI). Out of the five vibrations mentioned, the ν_4 and ν_5 vibrations were found to be IR active and also break the D_{3h} symmetry (see Figure **S4**). Here ν_4 corresponds to ∠N-M-N bond angle bending and correlates to Jahn-Teller active vibration (E′ irreducible representation in D_{3h} symmetry). The ν_5 corresponds to out-of-plane (M-N-N-N) bending vibration of the metal ion and associate with A_2" irreducible representation. Several displacement points in ν_4 and ν_5 vibrational surfaces were considered for CASSCF/NEVPT2 calculations. The maximum displacement scale of a particular vibration *j*, denoted by x_j, was fixed at 2.0 for both the complexes as suggested earlier (see Table **S6** and **S7** in ESI).[16]

An angular distortion parameter *Q* was introduced, which is a sum of deviation from 120° from each of the equatorial ∠N-M-N angles (denoted as α) (see Table **S6** and **S7**).[6e] Here, in order to

find out the spin-vibronic coupling, the variation of D and E/D have been computed with respect to the displacement of nuclear coordinates (x) using the following Hamiltonian:

$$\widehat{H}_{s-vib} = (\frac{\partial D}{\partial x})x\left[S_Z^2 - \frac{S(S+1)}{3}\right] + (\frac{\partial E}{\partial x})x(S_x^2 - S_y^2) \ldots eqn. 1)$$

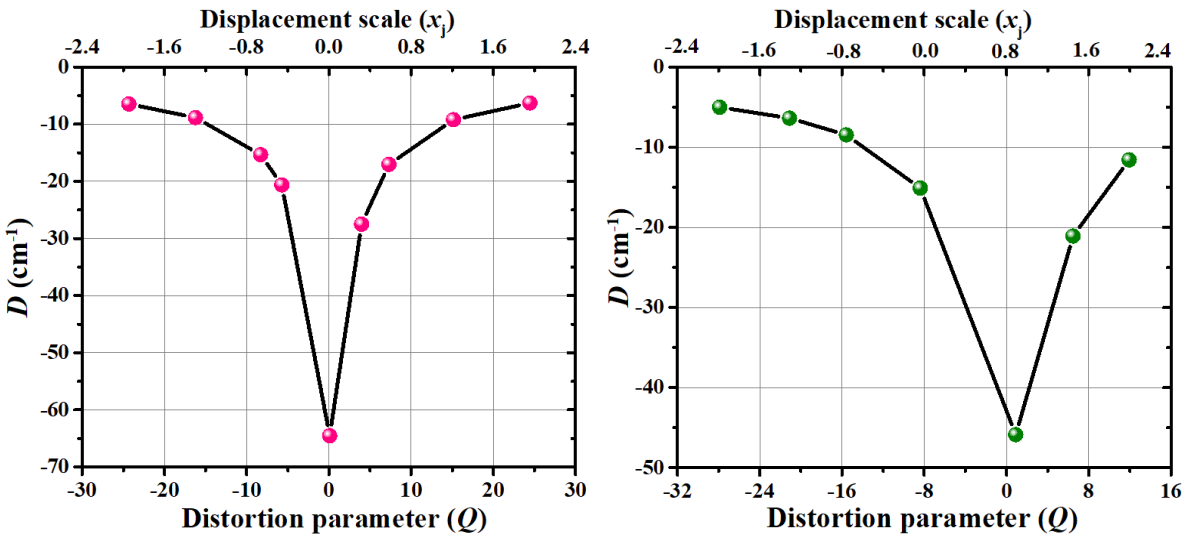

Figure 3: Variation of D values in complexes **1** (left) and **2** (right) with respect to the distortion parameter Q and displacement factor x_j for ν_4 vibrational mode.

In Figure **3**, we plot computed D values with respect to Q and x_j, and these plots show that as the Q diverges from zero, the magnitude of D decreases for ν_4 vibrations (see Figure **S5** in ESI). This is because an increase in Q breaks the D_{3h} symmetry and, consequently, increases the gap between the d_{xy} and $d_{x^2-y^2}$ orbitals (see Fig. **S6**). In complex **1**, the X-Ray structure shows the highest negative D value and minimum E/D value (see Fig. **S5**) at equilibrium geometry or zero displacement point, but for complex **2**, the X-ray structure is significantly deviated from the ideal D_{3h} symmetry and therefore do not have the largest negative D or the lowest E/D at zero

displacement point. In complex **2**, at x_j = 0.8 (see Fig. **3**), the *Q* parameter shows a minimum and predicts a *D* value as high as -46 cm^{-1}.

Furthermore, we have developed a three-dimensional magneto-structural correlation to see the effect of angle change on the *D* values for complex **1** and **2** (see Figure **4** and **S7** in ESI). It is very clear that the *D* is maximum when all the three equatorial angles are 120°. For **1**, the variation in *D* values is found to be relatively smaller for ν_5 vibrations compared to ν_4 mode (see Table **S8-S9** in ESI). For **2** no spin-vibrational coupling is detected as a much smaller change in *D* is noted. To rationalize this observation, the AILFT computed d-orbitals are plotted, and this reveals that the d_{xy}-$d_{x^2-y^2}$ orbital energy gap is altered only slightly in **1** and negligibly in **2** (see Fig. **S8-S9**). This suggests that ν_4 vibrational mode is dominant in controlling the magnetic anisotropy in trigonal planar d^4 systems, and this vibration likely offers a smaller barrier height for relaxation at lower temperatures. Between complex **1** and **2**, the spin-vibronic coupling is found to be stronger in the former.

At the equilibrium geometries, neglecting other effects, the computed U_{cal} values for complexes **1** and **2** are 153.8 and 44.7 cm^{-1} for complexes **1** and **2,** respectively. Considering the vibrational relaxation ν_4 modes at the displacement scale of x_j=±2, the U_{eff} value is expected to be diminished to 19 cm^{-1} and 15 cm^{-1} for complexes **1** and **2**, respectively (neglecting the QTM effects). This is substantially smaller than the barrier height estimated from the Orbach process and suggests a dominant spin-vibrational relaxation role in the magnetization relaxation in these complexes. This may be attributed to the fact that the ∠N-M-N bond angle bending vibration is very subtle and does not require significant energy for structural distortion and is strongly correlated to the d_{xy} and $d_{x^2-y^2}$ gap altering the magnetic anisotropy. This advocates a design principle that a rigid structure

with a robust N-Mn-N angle could block such relaxation, and this is possible if a chelate type or macrocyclic type ligands are employed.

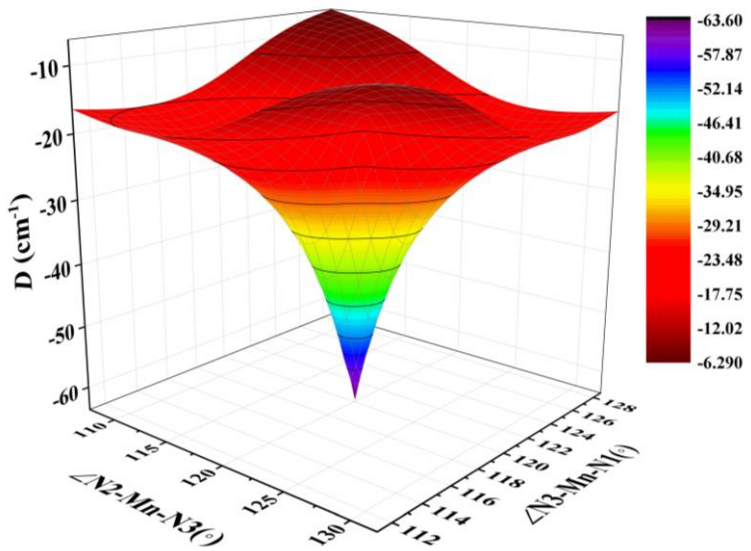

Figure **4**. Three-dimensional magneto-structural correlation of *D* obtained from ν_4 mode for complex **1**.

Conclusion

To the end, we have successfully employed an accurate *ab initio* method to explore the zero-field splitting and ligand field parameters in two Mn^{III} and Cr^{II} high spin complexes. A record-high *D* value of -64 cm^{-1} and -15 cm^{-1} was found for the X-ray structures of **1** and **2,** respectively. These two values are higher than any other reported *D* values for any mononuclear d^4 systems (see Table **S10** in ESI). While a significant barrier for magnetization relaxation is found for both the complexes, our detailed analysis revealed a strong spin-vibration coupling both the complexes that are likely to yield smaller blocking temperatures.

ASSOCIATED CONTENT

The following files are available free of charge.

AUTHOR INFORMATION

Corresponding Author

Gopalan Rajaraman. Email: rajaraman@chem.iitb.ac.in

Present Addresses

†Department of Chemistry, Indian Institute of Technology Bombay, Mumbai- 400076, Maharashtra, India

Author Contributions

The manuscript was written through contributions of all authors. All authors have given approval to the final version of the manuscript.

Funding Sources

This work was funded by DST and SERB (CRG/2018/000430; DST/SJF/CSA-03/2018-10; SB/SJF/2019-20/12), UGC-UKIERI (184-1/2018(IC)) and SUPRA (SPR/2019/001145).

ACKNOWLEDGMENT

RJ thanks DST-INSPIRE and AS thanks IIT Bombay for IPDF funding.

REFERENCES

1. (a) Sessoli, R.; Gatteschi, D.; Caneschi, A.; Novak, M., Magnetic bistability in a metal-ion cluster. *Nature* **1993,** *365* (6442), 141-143; (b) Gatteschi, D.; Sessoli, R.; Villain, J., *Molecular nanomagnets*. Oxford University Press on Demand: 2006; Vol. 5.

2. Woodruff, D. N.; Winpenny, R. E.; Layfield, R. A., Lanthanide single-molecule magnets. *Chem. Rev.* **2013,** *113* (7), 5110-5148.

3. Gomez-Coca, S.; Cremades, E.; Aliaga-Alcalde, N.; Ruiz, E., Mononuclear single-molecule magnets: tailoring the magnetic anisotropy of first-row transition-metal complexes. *J. Am. Chem. Soc.* **2013,** *135* (18), 7010-8.

4. (a) Gomez-Coca, S.; Urtizberea, A.; Cremades, E.; Alonso, P. J.; Camon, A.; Ruiz, E.; Luis, F., Origin of slow magnetic relaxation in Kramers ions with non-uniaxial anisotropy. *Nat. Commun.* **2014,** *5*, 4300; (b) Rechkemmer, Y.; Breitgoff, F. D.; van der Meer, M.; Atanasov, M.; Hakl, M.; Orlita, M.; Neugebauer, P.; Neese, F.; Sarkar, B.; van Slageren, J., A four-coordinate cobalt(II) single-ion magnet with coercivity and a very high energy barrier. *Nat. Commun.* **2016,** *7*, 10467; (c) Escalera-Moreno, L.; Suaud, N.; Gaita-Arino, A.; Coronado, E., Determining Key Local Vibrations in the Relaxation of Molecular Spin Qubits and Single-Molecule Magnets. *J. Phys. Chem. Lett.* **2017,** *8* (7), 1695-1700; (d) Lunghi, A.; Totti, F.; Sessoli, R.; Sanvito, S., The role of anharmonic phonons in under-barrier spin relaxation of single molecule magnets. *Nat. Commun.* **2017,** *8*, 14620; (e) Moseley, D. H.; Stavretis, S. E.; Thirunavukkuarasu, K.; Ozerov, M.; Cheng, Y.; Daemen, L. L.; Ludwig, J.; Lu, Z.; Smirnov, D.; Brown, C. M.; Pandey, A.; Ramirez-Cuesta, A. J.; Lamb, A. C.; Atanasov, M.; Bill, E.; Neese, F.; Xue, Z. L., Spin-phonon couplings in transition metal complexes with slow magnetic relaxation. *Nat. Commun.* **2018,** *9* (1), 2572.

5. Abragam, A.; Bleaney, B., *Electron paramagnetic resonance of transition ions*. OUP Oxford: 2012.

6. (a) Zadrozny, J. M.; Xiao, D. J.; Atanasov, M.; Long, G. J.; Grandjean, F.; Neese, F.; Long, J. R., Magnetic blocking in a linear iron (I) complex. *Nat. Chem.* **2013,** *5* (7), 577; (b) Zadrozny, J. M.; Atanasov, M.; Bryan, A. M.; Lin, C.-Y.; Rekken, B. D.; Power, P. P.; Neese, F.; Long, J. R., Slow magnetization dynamics in a series of two-coordinate iron (II) complexes. *Chem. Sci.* **2013,** *4* (1), 125-138; (c) Yao, X.-N.; Du, J.-Z.; Zhang, Y.-Q.; Leng, X.-B.; Yang, M.-W.; Jiang, S.-D.; Wang, Z.-X.; Ouyang, Z.-W.; Deng, L.; Wang, B.-W., Two-coordinate Co (II) imido complexes as outstanding single-molecule magnets. *J. Am. Chem. Soc.* **2016,** *139* (1), 373-380; (d) Bunting, P. C.; Atanasov, M.; Damgaard-Møller, E.; Perfetti, M.; Crassee, I.; Orlita, M.; Overgaard, J.; Van Slageren, J.; Neese, F.; Long, J. R., A linear cobalt (II) complex with maximal orbital angular momentum from a non-Aufbau ground state. *Science* **2018,** *362* (6421), eaat7319; (e) Craig, G. A.; Sarkar, A.; Woodall, C. H.; Hay, M. A.; Marriott, K. E. R.; Kamenev, K. V.;

Moggach, S. A.; Brechin, E. K.; Parsons, S.; Rajaraman, G.; Murrie, M., Probing the origin of the giant magnetic anisotropy in trigonal bipyramidal Ni(ii) under high pressure. *Chem. Sci.* **2018,** *9* (6), 1551-1559; (f) Sarkar, A.; Dey, S.; Rajaraman, G., Role of coordination number and geometry in controlling the magnetic anisotropy in FeII, CoII, and NiII single-ion magnets. *Chem. Eur. J* **2020,** *26*, 14036-14058.

7. Ako, A. M.; Hewitt, I. J.; Mereacre, V.; Clérac, R.; Wernsdorfer, W.; Anson, C. E.; Powell, A. K., A ferromagnetically coupled Mn19 aggregate with a record S= 83/2 ground spin state. *Angewandte Chemie* **2006,** *118* (30), 5048-5051.

8. (a) Maurice, R.; de Graaf, C.; Guihery, N., Magnetostructural relations from a combined ab initio and ligand field analysis for the nonintuitive zero-field splitting in Mn(III) complexes. *The Journal of chemical physics* **2010,** *133* (8), 084307; (b) Ishikawa, R.; Miyamoto, R.; Nojiri, H.; Breedlove, B. K.; Yamashita, M., Slow relaxation of the magnetization of an Mn(III) single ion. *Inorg. Chem.* **2013,** *52* (15), 8300-2; (c) Vallejo, J.; Pascual-Alvarez, A.; Cano, J.; Castro, I.; Julve, M.; Lloret, F.; Krzystek, J.; De Munno, G.; Armentano, D.; Wernsdorfer, W.; Ruiz-Garcia, R.; Pardo, E., Field-induced hysteresis and quantum tunneling of the magnetization in a mononuclear manganese(III) complex. *Angewandte Chemie* **2013,** *52* (52), 14075-9; (d) Chen, L.; Wang, J.; Liu, Y.-Z.; Song, Y.; Chen, X.-T.; Zhang, Y.-Q.; Xue, Z.-L., Slow Magnetic Relaxation in Mononuclear Octahedral Manganese(III) Complexes with Dibenzoylmethanide Ligands. *Eur. J. Inorg. Chem.* **2015,** *2015* (2), 271-278; (e) Craig, G. A.; Marbey, J. J.; Hill, S.; Roubeau, O.; Parsons, S.; Murrie, M., Field-induced slow relaxation in a monometallic manganese(III) single-molecule magnet. *Inorg. Chem.* **2015,** *54* (1), 13-5; (f) Pascual-Alvarez, A.; Vallejo, J.; Pardo, E.; Julve, M.; Lloret, F.; Krzystek, J.; Armentano, D.; Wernsdorfer, W.; Cano, J., Field-Induced Slow Magnetic Relaxation in a Mononuclear Manganese(III)-Porphyrin Complex. *Chemistry* **2015,** *21* (48), 17299-307; (g) Duboc, C., Determination and prediction of the magnetic anisotropy of Mn ions. *Chem. Soc. Rev.* **2016,** *45* (21), 5834-5847; (h) Realista, S.; Fitzpatrick, A. J.; Santos, G.; Ferreira, L. P.; Barroso, S.; Pereira, L. C.; Bandeira, N. A.; Neugebauer, P.; Hruby, J.; Morgan, G. G.; van Slageren, J.; Calhorda, M. J.; Martinho, P. N., A Mn(iii) single ion magnet with tridentate Schiff-base ligands. *Dalton Trans.* **2016,** *45* (31), 12301-7; (i) Sanakis, Y.; Krzystek, J.; Maganas, D.; Grigoropoulos, A.; Ferentinos, E.; Kostakis, M. G.; Petroulea, V.; Pissas, M.; Thirunavukkuarasu, K.; Wernsdorfer, W., Magnetic Properties and Electronic Structure of the S= 2 Complex [MnIII {(OPPh2) 2N} 3] Showing Field-Induced Slow Magnetization Relaxation. *Inorg. Chem.* **2020,** *59* (18), 13281-13294.

9. Neese, F., Software update: the ORCA program system, version 4.0. *WIRES: Comp. Mol. Sci.* **2018,** *8* (1), e1327.

10. Ellison, J. J.; Power, P. P.; Shoner, S. C., First examples of three-coordinate manganese (III) and cobalt (III): synthesis and characterization of the complexes M [N (SiMe3) 2] 3 (M= Mn or Co). *J. Am. Chem. Soc.* **1989,** *111* (20), 8044-8046.

11. Wagner, C. L.; Phan, N. A.; Fettinger, J. C.; Berben, L. A.; Power, P. P., New Characterization of V{N(SiMe3)2}3: Reductions of Tris[bis(trimethylsilyl)amido]vanadium(III)

and -chromium(III) To Afford the Reduced Metal(II) Anions [M{N(SiMe3)2}3](-) (M = V and Cr). *Inorg. Chem.* **2019,** *58* (9), 6095-6101.
12. Maurice, R.; Bastardis, R.; Graaf, C. d.; Suaud, N.; Mallah, T.; Guihery, N., Universal theoretical approach to extract anisotropic spin Hamiltonians. *J. Chem. Theory Comput.* **2009,** *5* (11), 2977-2984.
13. Singh, S. K.; Eng, J.; Atanasov, M.; Neese, F., Covalency and chemical bonding in transition metal complexes: An ab initio based ligand field perspective. *Coord. Chem. Rev.* **2017,** *344*, 2-25.
14. Frisch, M.; Trucks, G.; Schlegel, H. B.; Scuseria, G. E.; Robb, M. A.; Cheeseman, J. R.; Scalmani, G.; Barone, V.; Mennucci, B.; Petersson, G., gaussian 09, Revision d. 01, Gaussian. *Inc., Wallingford CT* **2009,** *201*.
15. (a) Schäfer, A.; Horn, H.; Ahlrichs, R., Fully optimized contracted Gaussian basis sets for atoms Li to Kr. *J. Chem. Phys.* **1992,** *97* (4), 2571-2577; (b) Schäfer, A.; Huber, C.; Ahlrichs, R., Fully optimized contracted Gaussian basis sets of triple zeta valence quality for atoms Li to Kr. *J. Chem. Phys.* **1994,** *100* (8), 5829-5835.
16. Goodwin, C. A.; Ortu, F.; Reta, D.; Chilton, N. F.; Mills, D. P., Molecular magnetic hysteresis at 60 kelvin in dysprosocenium. *Nature* **2017,** *548* (7668), 439.

TOC: Using Ab initio NEVPT2 calculations, we offer a design principle to enhance ZFS in high-spin d4 complexes of first-row transition elements.